PNAS
www.pnas.org

Supplementary Information for

Structural insight into TRPV5 channel function and modulation

Shangyu Dang[1], Mark K. van Goor[1,2], Daniel Asarnow[1], YongQiang Wang[1], David Julius[3*], Yifan Cheng[1,4*] and Jenny van der Wijst[1,2*]

[1]Department of Biochemistry and Biophysics, University of California San Francisco, San Francisco, CA, USA
[2]Department of Physiology, Radboud Institute for Molecular Life Sciences, Radboud university medical center, Nijmegen, The Netherlands
[3]Department of Physiology, University of California, San Francisco, California, 94143, USA
[4]Howard Hughes Medical Institute, University of California San Francisco, San Francisco, CA, USA

Correspondence to:
Jenny van der Wijst, PhD
Email: jenny.vanderwijst@radboudumc.nl
Yifan Cheng, PhD
Email: yifan.cheng@ucsf.edu
David Julius, PhD
Email: David.Julius@ucsf.edu

This PDF file includes:

Figs. S1 to S11
Table S1

www.pnas.org/cgi/doi/10.1073/pnas.1820323116

Supplemental figures

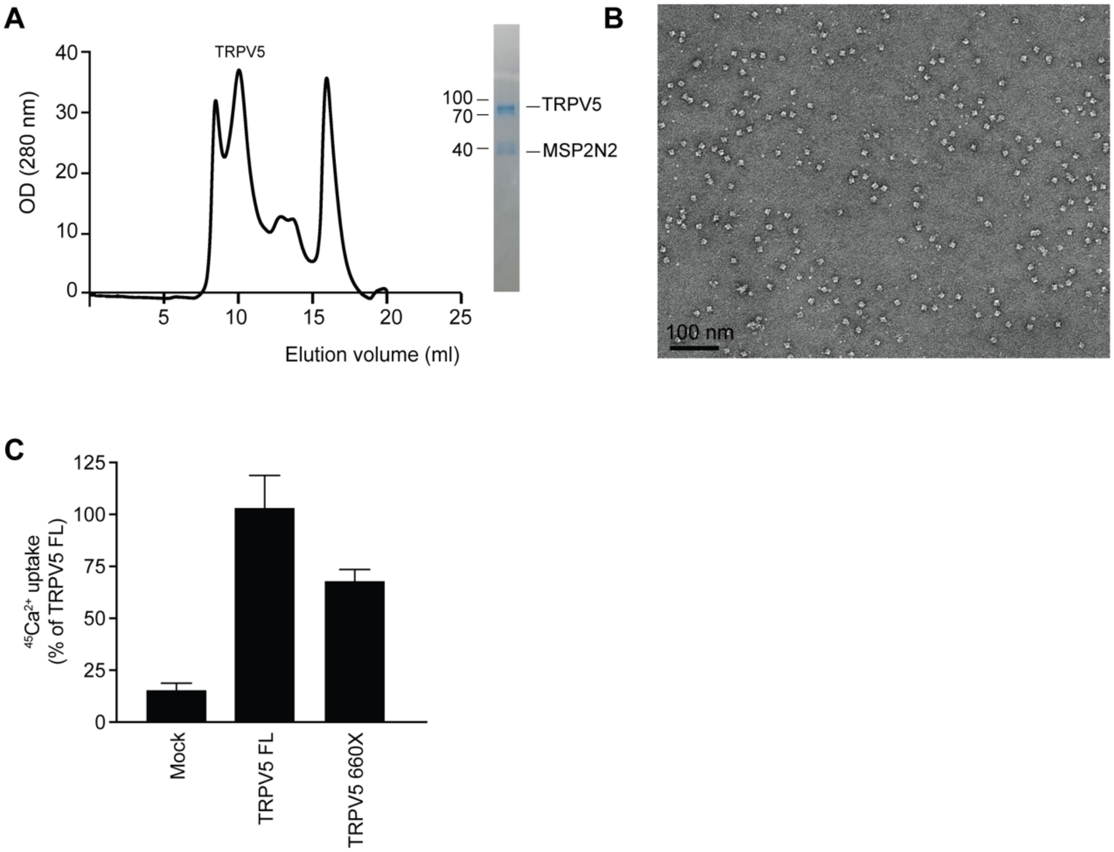

Fig. S1. Lipid nanodisc reconstitution and function of TRPV5. (A) Size-exclusion profile of nanodisc-reconstituted TRPV5 1-660 after proteolytic removal of the MBP tag. Insert: Coomassie blue staining of the TRPV5-nanodisc complex peak. (B) Representative negative stain image of purified TRPV5 1-660. (C) Radioactive ^{45}Ca uptake assay of HEK293 cells transfected with mock, full-length TRPV5, and C-truncated (660X) TRPV5. Uptake is shown as the mean+/-SEM (N=3).

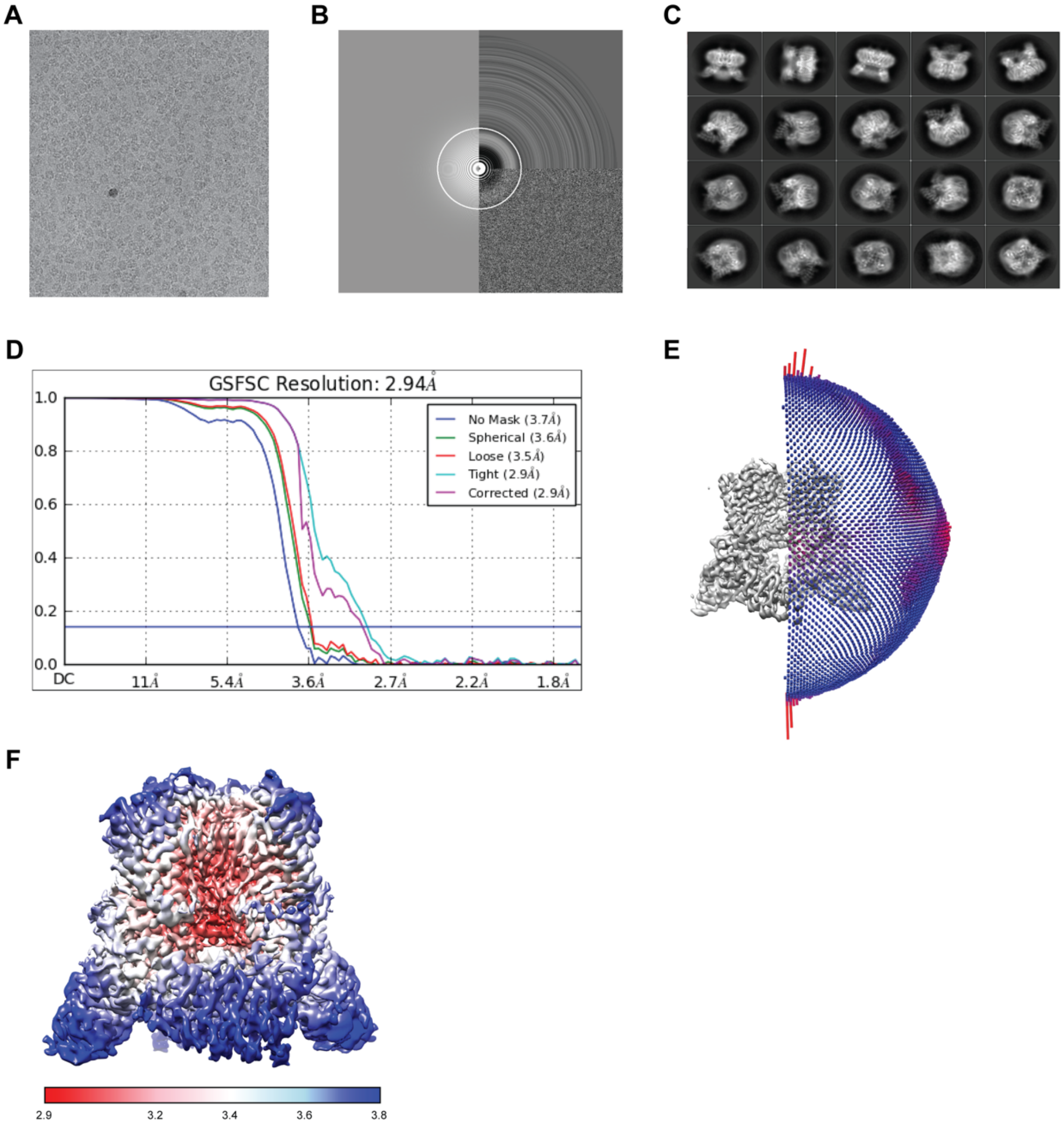

Fig. S2. Cryo-EM structure of TRPV5 1-660. (A) An example of an electron micrograph of TRPV5 1-660 in lipid nanodiscs. (B) Fourier power spectrum calculated from the micrograph shown in (A). (C) Representative 2D class averages calculated from selected particles. (D) FSC curves of the 3D reconstructions of the entire molecule as a tetramer with imposed C4 symmetry. (E) Euler angle distributions of all particles used in the final nanodisc-stabilized TRPV5 3D reconstruction. (F) Side view of the density map, colored according to the local resolution estimation made by Resmap.

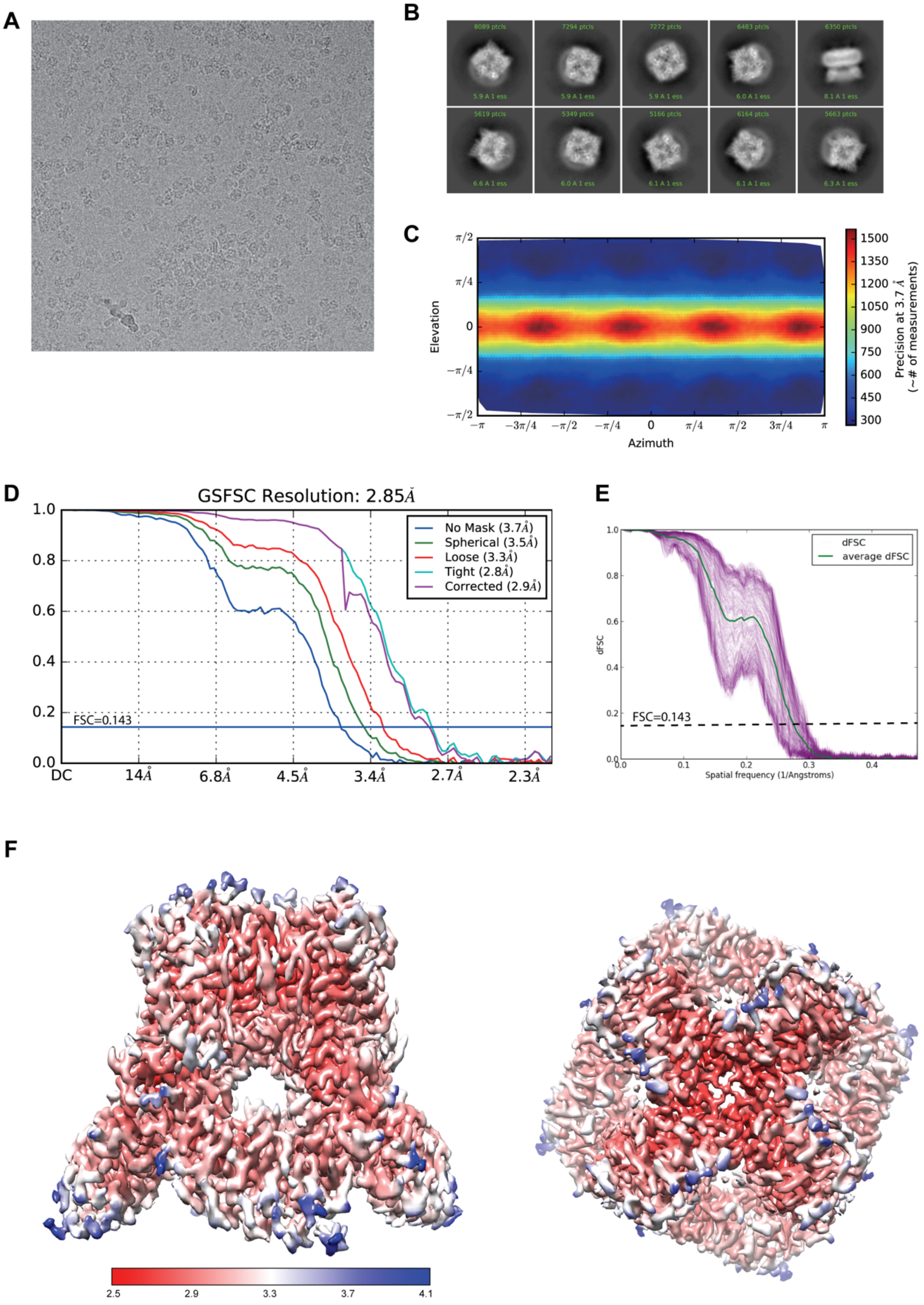

Fig. S3. Cryo-EM structure of TRPV5 W583A. (A) An example of an electron micrograph of TRPV5 W583A in lipid nanodiscs. (B) Representative 2D class averages calculated from selected particles. (C) Posterior precision directional distributions of all particles used in the final 3D reconstruction.

(D) FSC curves of the 3D reconstructions of the entire molecule as a tetramer with imposed C4 symmetry. (E) Directional FSC from different Fourier cones. Each curve indicates a different direction. (F) Side view and bottom view of the density map, colored according to the local resolution estimation made by Resmap.

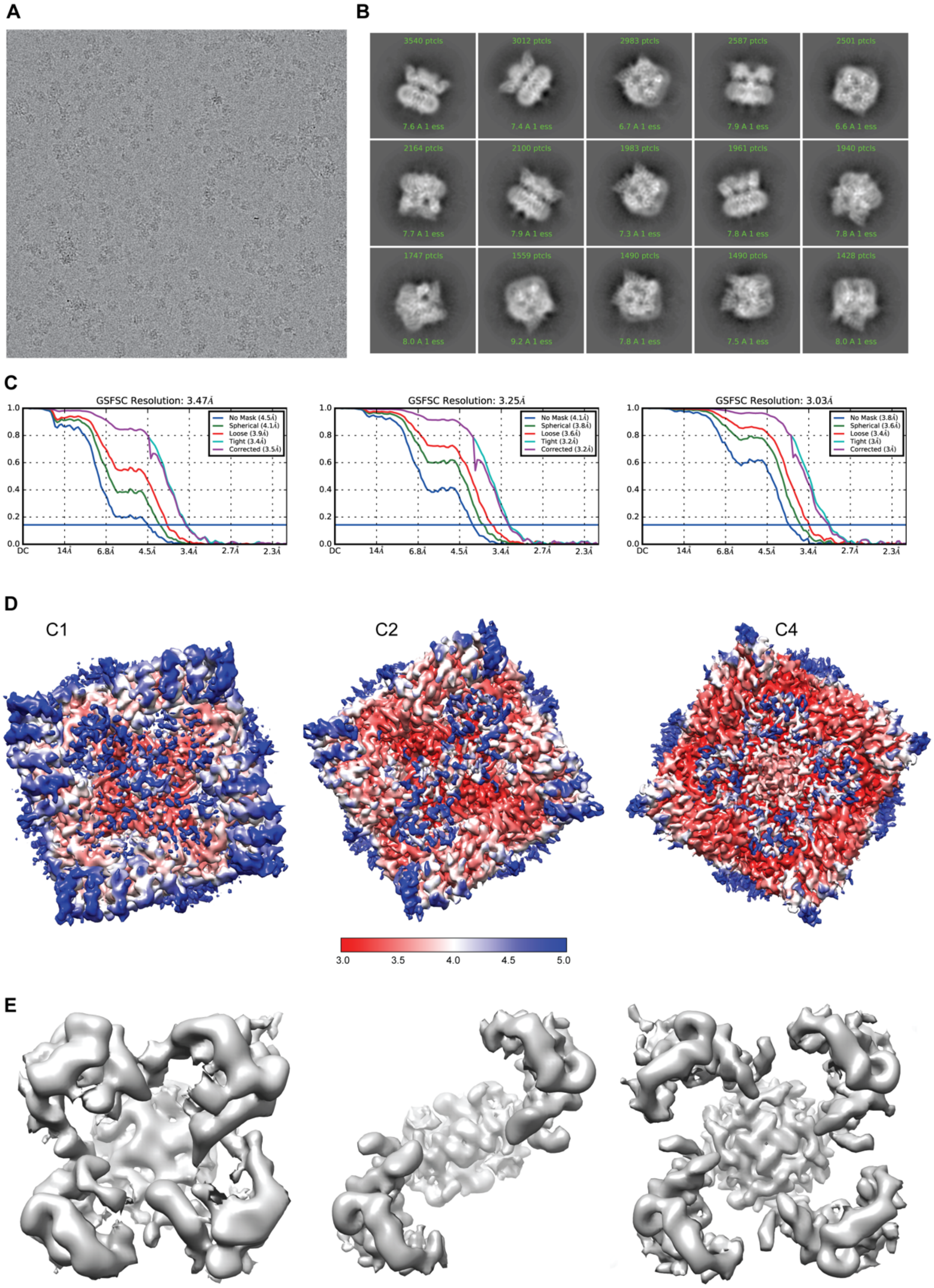

Fig. S4. Cryo-EM structure of TRPV5-CaM. (A) An example of an electron micrograph of TRPV5-CaM complex in LMNG. (B) Representative 2D class averages calculated from selected particles. (C) Posterior precision directional distributions of all particles used in the final 3D reconstruction for C1, C2 and C4 refinement respectively. (D) Bottom view of the density map in order to show CaM density clearly, for C1, C2 and C4 refinement respectively, colored according to the local resolution estimation made by Resmap. (E) Bottom views of the density map with CaM density isolated, with C1, C2 and C4 symmetry applied during the refinement.

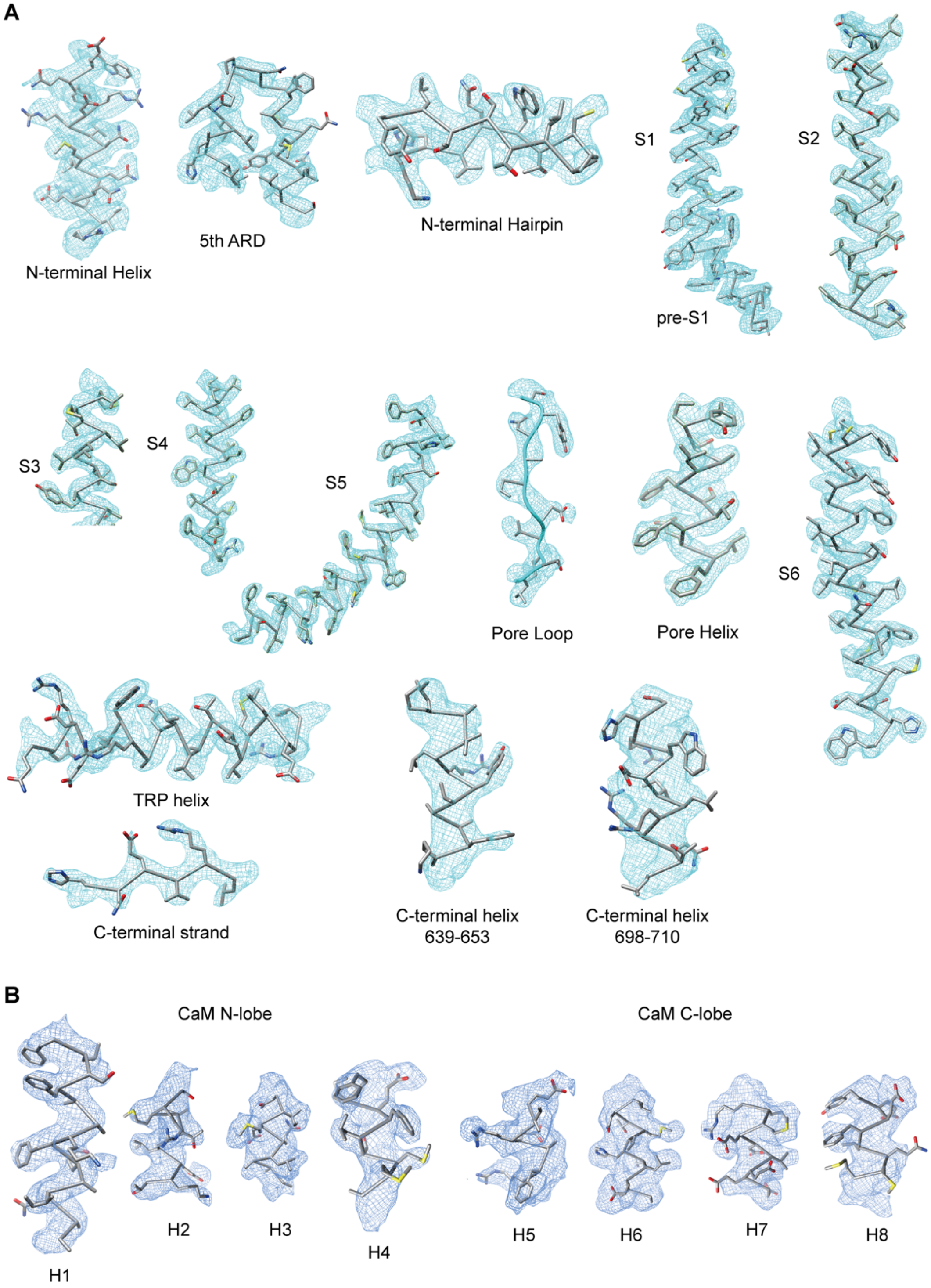

Fig. S5. Cryo-EM densities of TRPV5-CaM. (A,B) Fragments of the helical domains of TRPV5 (A) and CaM (B). The density is shown as blue mesh and the corresponding structural model in grey with side chains of residues depicted to demonstrate the quality of the map from various regions of the reconstructions.

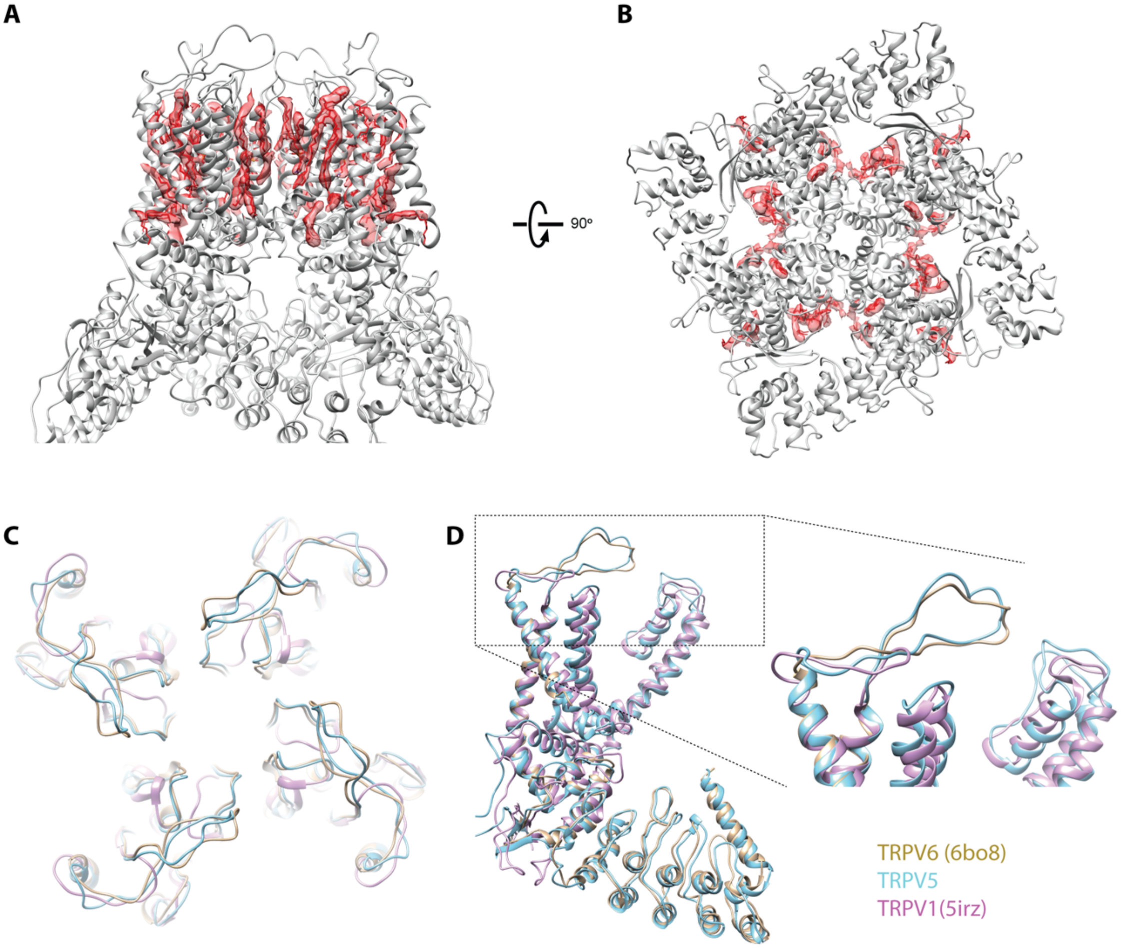

Fig. S6. Lipid densities and S1-S2 linker comparison. (A,B) Side and top view of the TRPV5 tetrameric complex, with lipid densities indicated in red. (C) top view overlay of the S1-S2 linker region of TRPV5 (cyan), TRPV6 (gold), and TRPV1 (purple). (D) comparison of the single monomers of TRPV5 (cyan), TRPV6 (gold), and TRPV1 (purple), with a zoomed insert of the outer pore region to indicate differences in the S1-S2 linker.

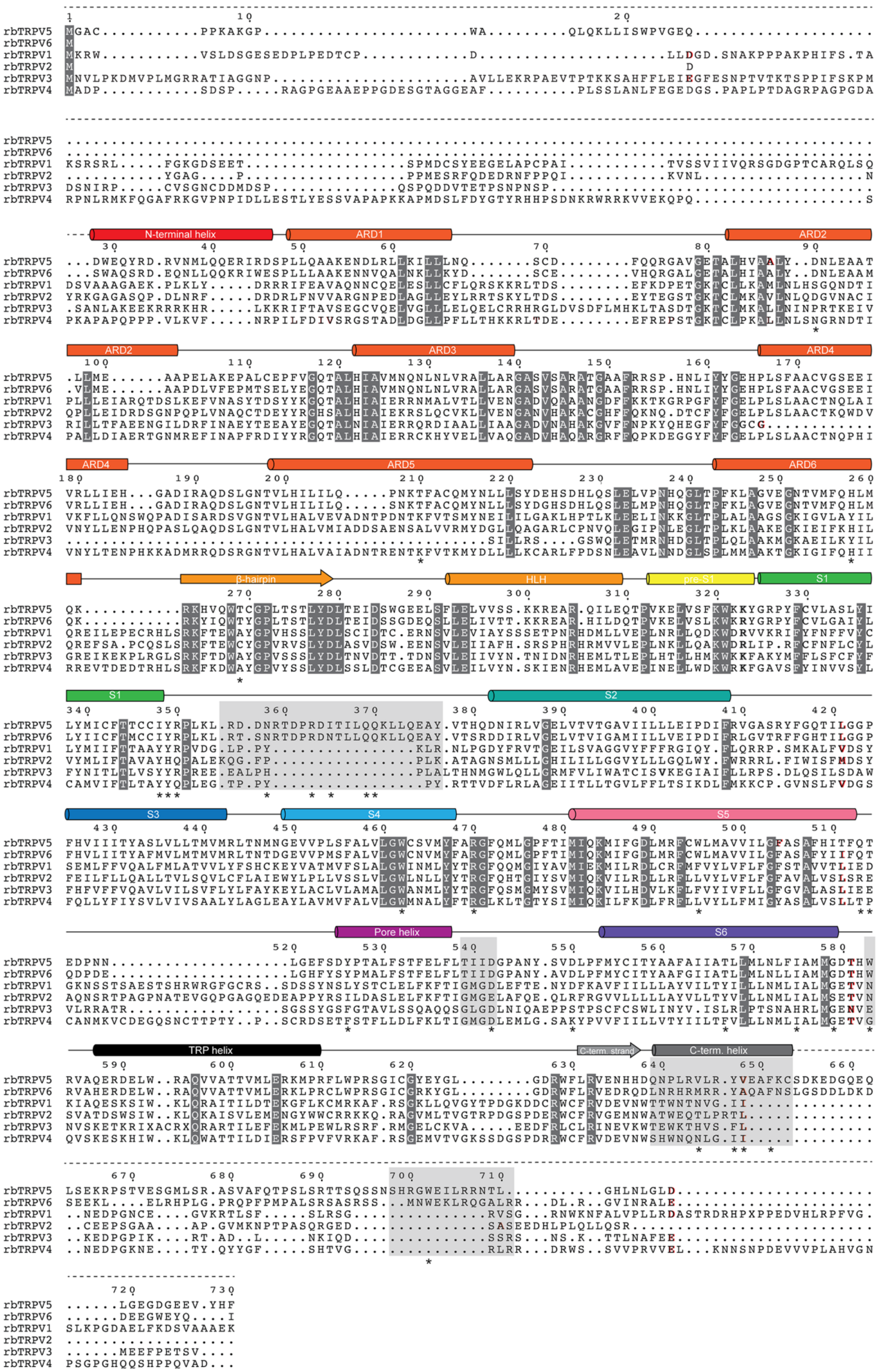
rbTRPV5
rbTRPV6
rbTRPV1
rbTRPV2
rbTRPV3
rbTRPV4
N-terminal helix
ARD1
ARD2
ARD3
ARD4
ARD5
ARD6
β-hairpin
HLH
pre-S1
S1
S2
S3
S4
S5
Pore helix
S6
TRP helix
C-term. strand
C-term. helix

Fig. S7. Sequence alignment of the TRPV family members. Complete sequence alignment of all rabbit members of the TRPV subfamily. Domains and corresponding secondary structures are marked according to rbTRPV5. Full conserved residues are marked by dark grey overlay and regions discussed in the main text are highlighted in light gray. Asterisks denote all residues that are mentioned in the main text.

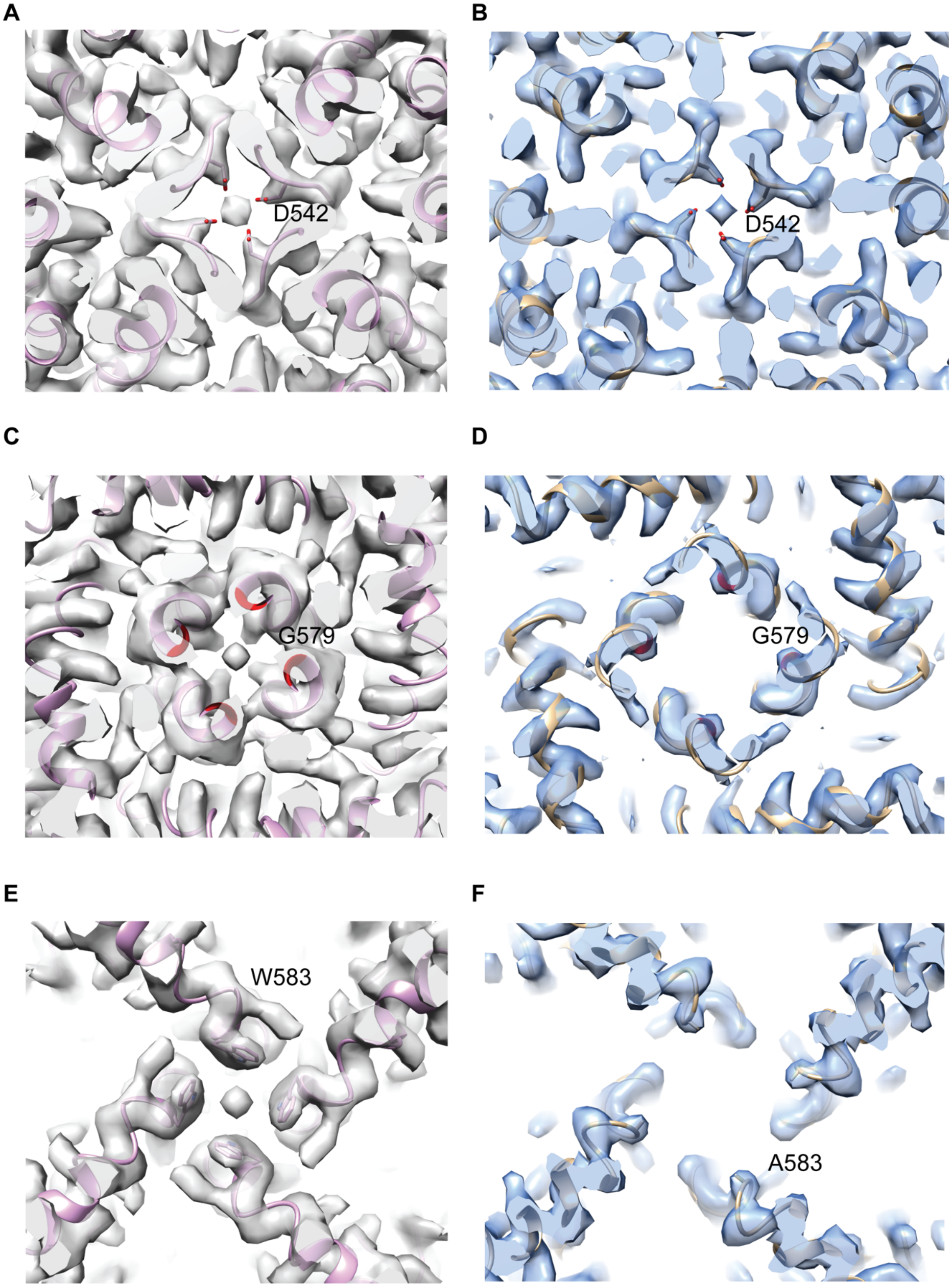

Fig. S8. Densities in the pore of TRPV5 1-660 and TRPV5 W583A. (A,B) Top view indicating the presence of the density in the selectivity filter of the nanodisc-reconstituted TRPV5 1-660 (A) and TRPV5 W583A (B). The side chains are visualized for D542. (C,D) Bottom view indicating the presence and absence of the density in nanodisc-reconstituted TRPV5 1-660 (C) and TRPV5

W583A (D), respectively. Residue G579 is projected in red. (E,F) Bottom view indicating the presence and absence of the density in nanodisc-reconstituted TRPV5 1-660 (E) and TRPV5 W583A (F), respectively. The side chains are visualized for the residues at the lower part of the pore, W583 (E) and A583 (F).

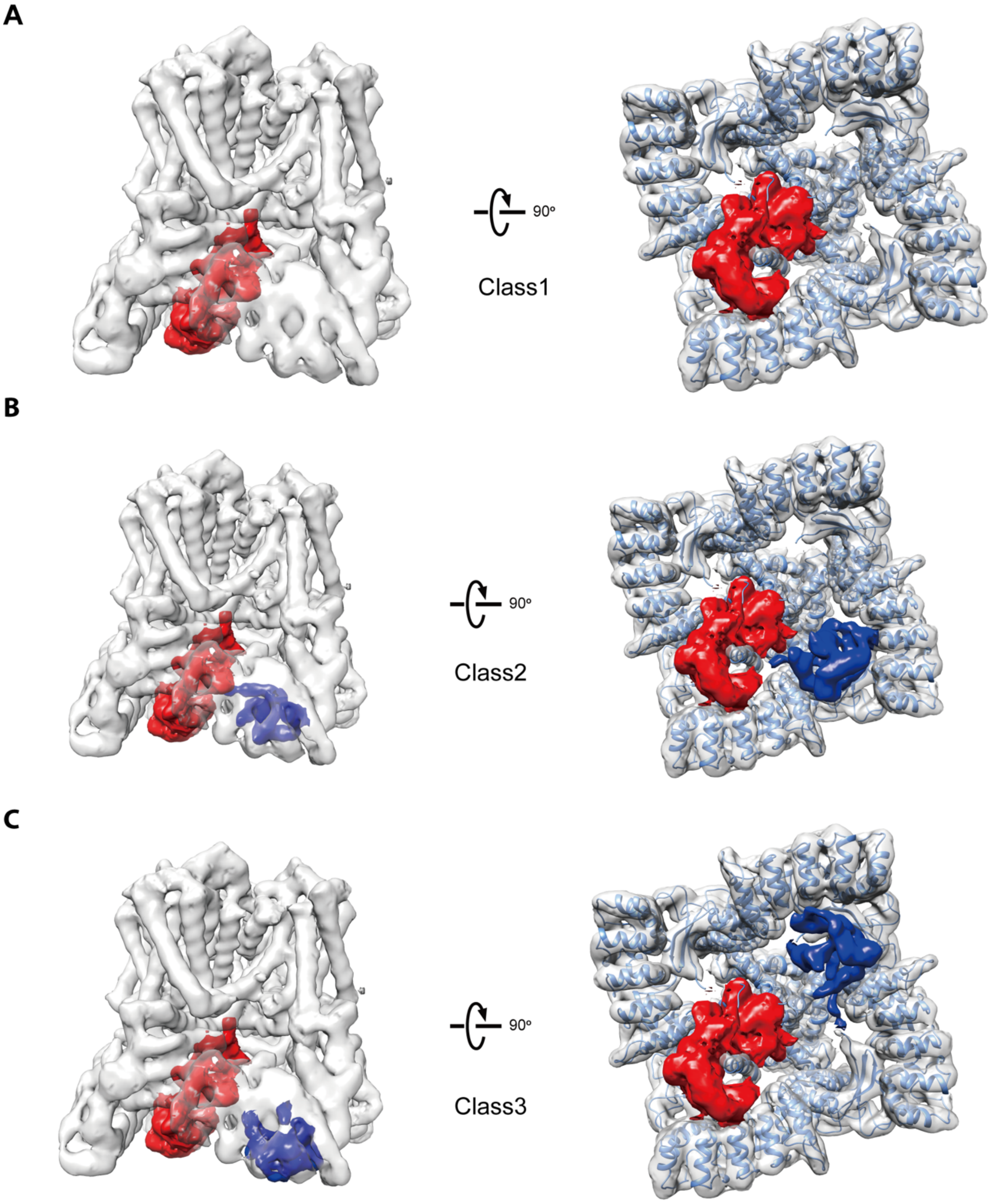

Fig. S9. Comparison of cryo-EM densities for TRPV5-CaM from different classes. (A-C) Front and bottom views of cryo-EM densities for TRPV5-CaM showing 3 different classes obtained after 3D classification in RELION. Extra densities belonging to CaM are indicated in red (N- and C-lobe) and blue (only N-lobe).

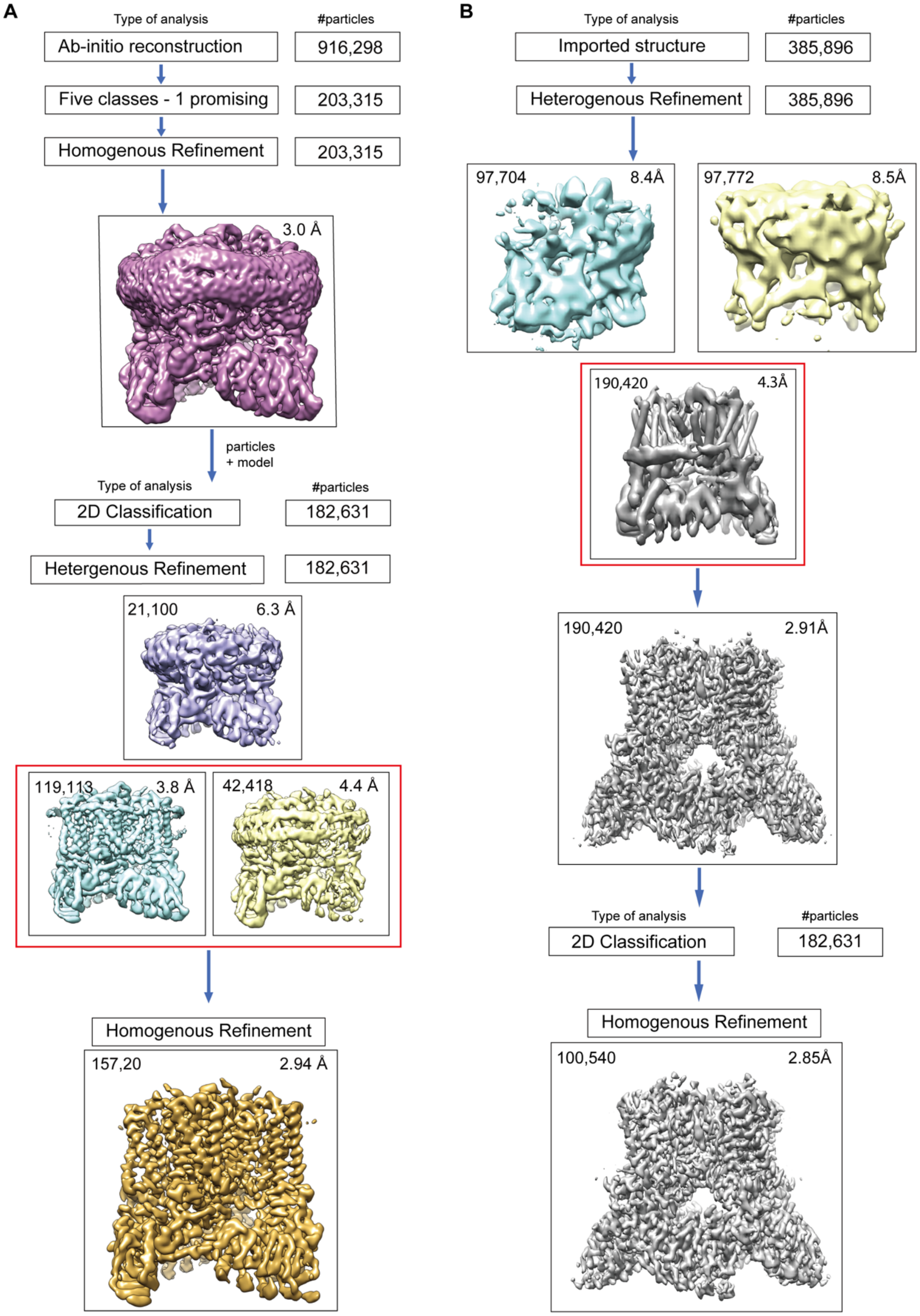

Fig. S10. Data processing and model building (A) Data processing workflow with the number of particles and the reconstruction resolutions of the TRPV5 1-660 sample indicated at every step. (B) Data processing workflow with the number of particles and the reconstruction resolutions of the TRPV5 W583A sample indicated at every step.

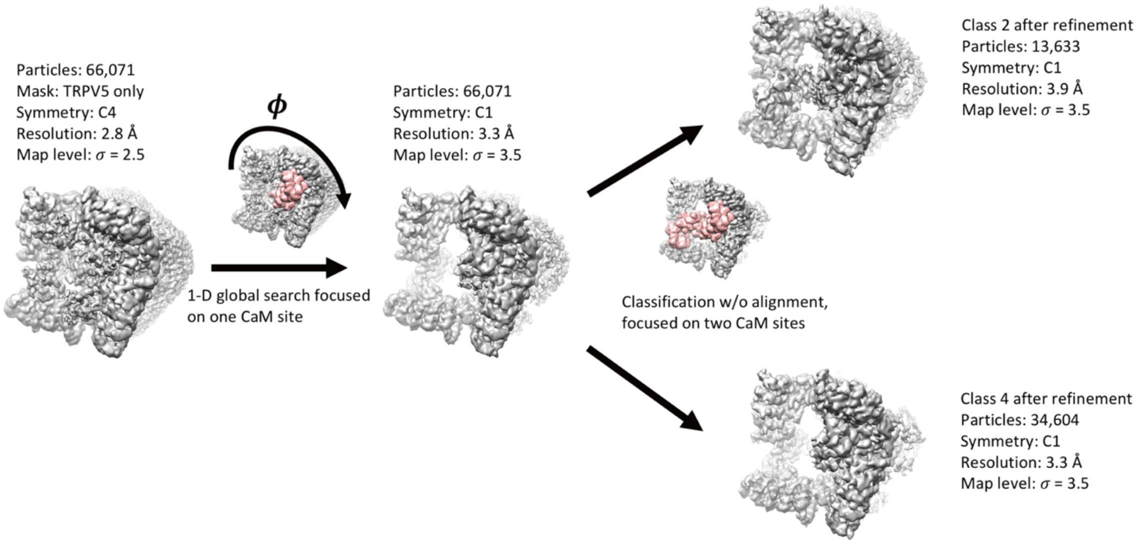

Fig. S11. Data process workflow of further alignment and classification. Bumber of particles, resolution and symmetry applied are indicated at every step.

Table S1. Summary of Cryo-EM Data Collection and Model Refinement

	1-660	**Full-length in ND**	**W583A**	**V5-CaM**
Data Collection/Processing				
Voltage (kV)	300	300	300	300
Magnification	130,000	22,500	22,500	22,500
Defocus Range (µm)	0.6 – 2.3	0.6 – 2.5	0.8 – 2.0	0.7 – 2.2
Pixel Size (Å)	0.84	1.059	1.059	1.059
Total Electron Dose (e^-/Å^2)	68	64	70	63
Exposure Time (s)	12	10	10	10
Number of Images	2968	930	1146	1135
Number of Frames/Image	60	50	50	50
Initial Particle Number	916,298	408,785	385,896	482,348
Final Particle Number	157,203	87,603	100,540	66,071
Resolution (unmasked, Å)	3.7	3.8	3.7	3.8/4.1/4.5*
Resolution (masked, Å)	2.9	3.0	2.8	3.0/3.2/3.3*

Refinement				
Number of Atoms	19584	19584	19612	20950
RMS Deviations				
Bond Lengths (Å)	0.010	0.011	0.010	0.008
Bond Angles (°)	1.262	1.366	1.076	1.082
Ramachandran				
Favored (%)	95.07	94.09	96.73	93.87
Allowed (%)	4.76	5.91	3.27	6.09
Outlier (%)	0.16	0.0	0.0	0.04
Molprobity Score	1.62	1.87	1.93	1.94
EMRinger Score	2.36	2.87	2.95	2.2

*Resolution shows refinement with C4/C2/C1 symmetry applied respectively.